Cite this: DOI: 10.1039/c0xx00000x

www.rsc.org/xxxxxx

ARTICLE TYPE

β-$BaGa[B_4O_8(OH)](H_2O)$ and $Ba_4Ga[B_{10}O_{18}(OH)_5](H_2O)$: New Barium Galloborates Featuring Unusual $[B_4O_8(OH)]^{5-}$ and $[B_{10}O_{18}(OH)_5]^{11-}$ Clusters

Hui Yang,[a,b] Chun-Li Hu,[a] Jun-Ling Song,[a] Jiang-Gao Mao*,[a]

Received (in XXX, XXX) Xth XXXXXXXXX 200X, Accepted Xth XXXXXXXXX 200X
DOI: 10.1039/b000000x

Two new barium galloborates, namely, *β*-$BaGa[B_4O_8(OH)](H_2O)$ (**1**) and $Ba_4Ga[B_{10}O_{18}(OH)_5](H_2O)$ (**2**), have been synthesized by hydrothermal reactions. Compounds **1** crystallizes in centrosymmetric space group *P*-1 and displays two-dimensional (2D) anionic layer composed of $[B_4O_8(OH)]^{5-}$ clusters and $[Ga_2O_8]^{10-}$ dimers interconnected by B–O–Ga linkages, furthermore Ba^{2+} ions and water molecules are located at the interlayer space. The neighbouring galloborate layers are connected via hydrogen bonds of water molecules. Compound **2** crystallizes in a polar space group *Cc*. In the structure, $[B_{10}O_{18}(OH)_5]^{11-}$ clusters and $[GaO_4]^{5-}$ tetrahedral are connected with each other to form a 3D network filled by Ba^{2+} ions and water molecules which consist of 1D tunnels based on unusual Ga_3B_{16} 19-member rings (MRs). The water molecules are coordinated with the Ba^{2+} ions and also form hydrogen bonds with the galloborate network. Second harmonic generation (SHG) measurements indicate that compound **2** displays a weak SHG response of about 0.2 times that of KH_2PO_4 (KDP). Optical properties, ferroelectric properties, piezoelectric property, thermal stability and theoretical calculations based on density functional theory (DFT) methods of both compounds have also been studied.

INTRODUCTION

During last few decades, second–order nonlinear optical (NLO) materials have attracted considerable attention because of their great practical application in photonic technologies.[1] Among them, borates have attracted a great deal of research attentions due to their rich structural chemistry, high damage threshold, and large nonlinear optical efficiency.[2] Many non–centrosymmetric borate crystals have been reported including *β*–BaB_2O_4 (BBO), LiB_3O_5 (LBO), and $KBeBO_3F_2$ (KBBF).[3] B atom can adopt two different basic coordination geometries: planar triangle with π-conjugated system (BO_3) and tetrahedron (BO_4). Furthermore, these BO_3 and BO_4 groups can be polymerized into a wide variety of anionic structures such as 1D chains, 2D sheets, or 3D networks in addition to isolated clusters.[4] Introduction of the heteroatom into the borate system has been proved to be an effective route for the preparations of new borates with novel topologies and enhanced second harmonic generation (SHG) properties. Recently, the family of metal borates have been expanded greatly to synthesize new classes of compounds such as borogermanates,[5] borophosphates,[6] aluminoborates,[7] borosulfates,[8] and boroberyllates.[9]

Coupled with the fact that Ga^{3+} ion can also form various coordination geometries such as GaO_4 tetrahedron, GaO_5 trigonal bipyramid and GaO_6 octahedron, we anticipate that the introduction of GaO_n (n = 4, 5, 6) groups into the borate systems can also result in a large number of galloborates with novel structures and excellent NLO properties. So far, a number of the alkali and alkaline-earth gallium borates have been studied.[10-20] The structurally characterized alkali metal galloborates include $LiGa(OH)(BO_3)(H_2O)$,[10] $A_2Ga(B_5O_{10})(H_2O)_4$ (A = Rb, K),[10,11] $K_2Ga_2O(BO_3)_2$,[12] $A_2Ga_2O(BO_3)_2$ (A = Na, K, Rb and Cs),[13] and $Li_6Ga_2B_4O_{12}$,[14] among which $Rb_2Ga(B_5O_{10})(H_2O)_4$ displays moderate strong SHG response of 1.0 × KDP (KH_2PO_4). A variety of alkaline earth metal galloborates have been also reported including $MgGaBO_4$,[15] $CaGaBO_4$,[16] two forms of $SrGaBO_4$,[16,17] $AeGa_2B_2O_7$ (Ae = Sr, Ba),[18] $BaGa[B_4O_8(OH)](H_2O)$[19] and $Ba_3Ga_2[B_3O_6(OH)]_2[B_4O_7(OH)_2]$ which displays moderately strong SHG response of 3.0 × KDP.[20] The structure of $BaGa_2B_2O_7$ consists of a framework structure of corner-sharing tetrahedral (GaO_4) chains and pyroborate (B_2O_5) groups with interspaces occupied by the eight-coordinated Ba^{2+} cations.[18] The structure of $BaGa[B_4O_8(OH)](H_2O)$ features a layered anionic framework composed of $[B_5O_9(OH)]$-like $[GaB_4O_{11}(OH)]$ clusters that are interconnected by Ga-O-Ga likages.[19] The structure of $Ba_3Ga_2[B_3O_6(OH)]_2[B_4O_7(OH)_2]$ exhibits a 3D networks with 14–member ring (MR) channels along the [100], [101], and [-101] directions based on GaO_4 tetrahedra, $B_3O_6(OH)$ and $B_4O_7(OH)_2$ clusters.[20]

The chemical compositions and structures of metal borates isolated are very sensitive to synthetic conditions such as temperature, the size and charge of cations, metal/borate ratio, pH value of the reaction media, etc. For example, $K_2[Ge(B_4O_9)]_2{\cdot}H_2O$, $K_4[B_8Ge_2O_{17}(OH)_2]$ and $KBGe_2O_6$ were isolated from the same system under different synthetic conditions.[21] With $K_2[B_4O_5(OH)]\cdot 2H_2O$ as a boron source and a mixture of water, pyridine and diethylenetriamine as solvent, $K_2[Ge(B_4O_9)]_2\cdot H_2O$ was obtained at 170 °C, whereas $K_4[B_8Ge_2O_{17}(OH)_2)]$ was prepared from a flux of $K_2[B_4O_5(OH)]\cdot 2H_2O$ at 280 °C. $KBGe_2O_6$ was prepared by using $K_2B_4O_7\cdot 4H_2O$ as a boron source in a mixture of water, ethylene glycol and 1,4-diazabicyclo[2, 2, 2]octane at 170 °C. We expect that the galloborate system will also be strongly affected by subtile changes of reaction conditions. Therefore, in order to further understand the relationship between the structures of the products formed and the reaction conditions, we started a research program to explore barium gallium borates systematically. Our research efforts led to the isolation of two new members in the Ba–Ga–B–O family, namely, *β*-$BaGa[B_4O_8(OH)](H_2O)$ (**1**) and $Ba_4Ga[B_{10}O_{18}(OH)_5](H_2O)$ (**2**). Herein, we report their syntheses, crystal structures, ferroelectric properties as well as optical properties.

Experimental Section

Materials and methods

H_3BO_3 (Shanghai Reagent Factory, 99.99%), Ga_2O_3 (Shanghai Reagent Factory, 99.99%), and $Ba(OH)_2\cdot 8H_2O$ (Alfa Aesar, 99.0%), $Na_2B_4O_7\cdot 10H_2O$ (Shanghai Reagent Factory, 99.99%), $BaSO_4$ (Alfa Aesar, 99.0%) were used without further purification. IR spectra were recorded on a Magna 750 FT–IR spectrometer as KBr pellets in the range of 4000–400 cm^{-1}. Microprobe elemental analyses were performed on a field–emission scanning electron microscope (JSM6700F) equipped with an energy–dispersive X–ray spectroscope (Oxford INCA). X–Ray powder diffraction (XRD) patterns were collected on a XPERT–MPD θ–2θ diffractometer using graphite–monochromated Cu-Kα radiation with a step size of 0.02 °. Optical diffuse–reflectance spectra were measured at room temperature with a PE Lambda 900 UV–visible spectrophotometer. The $BaSO_4$ plate was used as a standard (100% reflectance). The absorption spectrum was calculated from reflectance spectrum using the Kubelka–Munk function: $\alpha/S = (1-R)^2/2R$,[22] where α is the absorption coefficient, S is the scattering coefficient, which is practically wavelength–independent when the particle size is larger than 5 μm, and R is the reflectance. Thermogravimetric analyses (TGA) were carried out with a NETZSCH STA 449C unit at a heating rate of 10 °C/min under nitrogen atmosphere and differential scanning calorimetry (DSC) analyses were performed on a NETZSCH DTA404PC unit at heating rate of 10 °C/min under nitrogen atmosphere. Measurements of the powder frequency–doubling effect were carried out by means of the modified method of Kurtz and Perry.[23] A 1064 nm radiation generated by a Q–switched Nd:YAG solid–state laser was used as the fundamental frequency light. The SHG wavelength is 532 nm. Thus, the sample was ground and sieved into a specific particle size range (100–150 μm). Sieved KDP powder (100–150 μm) was used as a reference material to assume the SHG effect. The ferroelectric property for compound **2** was measured on an aixACCT TF Analyzer 2000E ferroelectric tester at room temperature and piezoelectric coefficient was measured by using a quasistatic d_{33} meter (Institute of Acoustics, Chinese Academy of Sciences, model ZJ-4AN). The powder was pressed into a pellet (5-mm-diameter and 0.4-mm-thick), and the conducting Ag-glue was applied on the both sides of the pellet surfaces for electrodes.

Synthesis of *β*-$BaGa[B_4O_8(OH)](H_2O)$ (1)

A mixture of $BaSO_4$ (0.0812 g, 0.35 mmol), Ga_2O_3 (0.0428 g, 0.22 mmol), and H_3BO_3 (0.1240 g, 2 mmol) in 3.0 mL H_2O with the pH value of 6.0 was sealed in an autoclave equipped with a Teflon liner (23 mL) and heated first at 100 °C for 5 h, and then 220 °C for 4 days followed by slow cooling to room temperature at a rate of 2.3 °C/h. The final pH value was close to 6.0. Colorless block crystals of compound **1** were collected in about 70% yield based on Ga. Its purity was confirmed by XRD powder diffraction study (Figure S1a in the ESI†). The average molar ratio of Ba: Ga in compound **1** determined by energy–dispersive spectrometry (EDS) on several single crystals is 1.2: 1, which is in good agreement with that determined from single–crystal X–ray structural studies. It is unsuccessful to synthesize compound **1** with other reactants like $Ba(OH)_2\cdot 8H_2O$ and $BaCl_2\cdot 2H_2O$. IR data (KBr cm^{-1}): 3441 (m), 1679 (m), 1410 (s), 1222 (s), 1034 (s), 921 (s), 853 (w), 740 (w), 658 (w).

Synthesis of $Ba_4Ga[B_{10}O_{18}(OH)_5](H_2O)$ (2)

A mixture of $Ba(OH)_2\cdot 8H_2O$ (0.3150 g, 1 mmol), Ga_2O_3 (0.0930 g, 0.5 mmol), H_3BO_3 (0.1240 g, 2 mmol) in 3.0 mL H_2O with the pH value of 14.0 was sealed in an autoclave equipped with a Teflon liner (23 mL) and heated at 100 °C for 5 h, then heated at 220 °C for 4 days followed by slow cooling to room temperature at a rate of 2.3 °C/h with the final pH value of 9.0. The product was washed with hot water and then dried in air. Colorless brick crystals of compound **2** were collected in about 30% yield based on Ga after sieving by ultrasound. Its purity was confirmed by XRD power diffraction studies (Figure S1b in the ESI†). The average molar ratio of Ba: Ga in compound **2** determined by energy–dispersive spectrometry (EDS) on several single crystals is 3.8: 1, which is in good agreement with that determined from single–crystal X–ray structural analyses. IR data (KBr cm^{-1}): 3405 (w), 1624 (w), 1341 (s), 1244 (w), 856 (m), 774 (w), 556 (w).

Single–crystal structure determination

Data collections for both compounds were performed on SuperNova (Mo) X–ray Source, Mo–Kα radiation (λ = 0.71073 Å) at 293(2) K. Both data sets were corrected for Lorentz and polarization factors as well as for absorption by the multi–scan method.[24a] Both structures were solved by direct methods and refined by a full–matrix least–squares fitting on F^2 by SHELX–97.[24b] All hydrogen atoms are located at geometrically calculated positions and refined with isotropic thermal parameters. The refined Flack factor of -0.02(7) for compound **2** is close to zero, confirming the correctness of its absolute structure. Both structures were also checked for possible missing symmetry with the program PLATON.[24c] Crystallographic data and structural refinements for the two compounds are summarized in Table 1 and important bond distances are listed in Table S1. More information about the crystallographic studies as well as atomic displacement parameters are given as electronic supporting information (ESI†). Further details of the crystal structure studies can be obtained from the FIZ Karlsruhe, 76344 Eggenstein-

Leopoldshafen, Germany (Fax: (49)7247808666; E-mail: crysdata@fiz-karlsruhe.de), on quoting the depository numbers CSD 427785, 427786.

Computational descriptions

Single crystal structural data of both compounds were used for the theoretical calculations. Band structures and density of states (DOS), and optical properties were performed with the total energy code CASTEP.[25] The total energy is calculated with density functional theory (DFT) using the Perdew–Burke–Ernzerhof in the generalized gradient approximation.[26] The interactions between the ionic cores and the electrons are described by the norm–conserving pseudopotential.[27] The following orbital electrons are treated as valence electrons: Ba–$5s^2 5p^6 6s^2$, Ga–$3d^{10} 4s^2 4p^1$, B–$2s^2 2p^1$, O–$2s^2 2p^4$ and H–$1s^1$. The number of plane waves included in the basis set is determined by a cut off energy of 800 eV. In addition, the numerical integration of the Brillouin zone is performed using a 4×4×3 and 4×2×1 Monkhorst–Pack *k*–point sampling for compounds **1** and **2**, respectively. The other calculating parameters and convergent criteria were the default values of the CASTEP code.

Result and discussion

Two new barium galloborates, namely, *β*–$BaGa[B_4O_8(OH)](H_2O)$ (**1**) and $Ba_4Ga[B_{10}O_{18}(OH)_5](H_2O)$ (**2**), were prepared by hydrothermal reactions. It is interesting to note that two compounds were synthesized under the same reaction temperature (220 °C) but different starting materials and molar ratios. *β*–$BaGa[B_4O_8(OH)](H_2O)$ (**1**) was prepared from a mixture of $BaSO_4$, Ga_2O_3, and H_3BO_3 with molar ratio of 1.7: 1: 10, whereas $Ba_4Ga[B_{10}O_{18}(OH)_5](H_2O)$ (**2**) was obtained from a mixture of $Ba(OH)_2{\cdot}8H_2O$, Ga_2O_3, and H_3BO_3 in a molar ratio of 2: 1: 4. It is interesting to note that the previously reported *α*–$BaGa[B_4O_8(OH)](H_2O)$ phase was prepared from a mixture of barium hydroxide, gallium isopropoxide, and boric acid (Ba/Ga/B molar ratio = 1.5: 1: 10) in a mixed solvent of water and pyridine at 260 °C.[19] $Ba_3Ga_2[B_3O_6(OH)]_2[B_4O_7(OH)_2]$ was isolated by hydrothermal reaction of a mixture of H_3BO_3, $Ga(iPrO)_3$ and $Ba(OH)_2$ (molar ratio= 4: 1: 2) in water at 220 °C for 10 days.[20] Hence the barium galloborates isolated are very sensitive to the gallium source, Ba/ Ga/ B molar ratio, reaction temperature and reaction media used. The structures of centrosymmetric *β*–$BaGa[B_4O_8(OH)](H_2O)$ (**1**) and polar $Ba_4Ga[B_{10}O_{18}(OH)_5](H_2O)$ (**2**) feature two different types of anionic open frameworks based on two types of borate clusters ($[B_4O_8(OH)]^{5-}$ and $[B_{10}O_{18}(OH)_5]^{11-}$) which are further interconnected by $[GaO_4]^{5-}$ or dimeric $[Ga_2O_8]^{10-}$ units, respectively. The polar compound **2** displays weak second–harmonic generation response of about 0.2 times of $K_2H_2PO_4$ (KDP).

Structural description. *β*–$BaGa[B_4O_8(OH)](H_2O)$ (**1**) crystallizes in the centrosymmetric space group *P*-1. Its structure features a layered anionic framework composed of $[B_4O_8(OH)]^{5-}$ clusters and $[Ga_2O_8]^{10-}$ dimers with Ba^{2+} ions and water molecules located at the interlayer space (Figure 1d), which is similar to that of *α*–$BaGa[B_4O_8(OH)](H_2O)$ which crystallizes in monoclinic space group *C*2/*c*.[19] The asymmetric unit of **1** contains one barium, one gallium, one $[B_4O_8(OH)]^{5-}$ cluster and a water molecule. The Ga^{3+} ion is five coordinated with a trigonal–bipyramidal coordination geometry. A pair of GaO_5 units forms a $[Ga_2O_8]^{10-}$ dimer via edge–sharing (O(8)–O(8)) (Figure 1b). The Ga–O distances range from 1.855(4) to 2.055(5) Å and O–Ga–O bond angles fall in the range from 77.7(2) and 170.48(1)°. Within the $[B_4O_8(OH)]^{5-}$ cluster, B(1), B(3) and B(4) atoms are three coordinated in a planar trigonal geometry whereas B(2) is tetrahedral coordinated. The B-O distances are in the range of 1.339(9) to 1.411(8) Å and 1.453(9) to 1.483(8) Å, and O–B–O bond angles range from 114.2(6) to 124.6(6)° and 105.3(5) to 111.7(5)° for BO_3 and BO_4 groups, respectively. These bond lengths and angles are comparable to those previously reported in *α*-$BaGa[B_4O_8(OH)](H_2O)$ and other related galloborates.[18–20] $B(2)O_4$, $B(3)O_3$ and $B(4)O_3$ form a common $[B_3O_7]^{5-}$ cluster via corner-sharing. The $B(1)O_3$ group is attached to the $[B_3O_7]^{5-}$ cluster by B(2)–O(3)–B(1) linkage, forming a $[B_4O_8(OH)]^{5-}$ anion (Figure 1a). The interconnection of $[B_4O_8(OH)]^{5-}$ clusters and $[Ga_2O_8]^{10-}$ dimers via B-O-Ga linkages result in a $[GaB_4O_8(OH)]^{2-}$ layer parallel to the *ab* plane (Figure 1c). The interlayer distance is about 9.84 Å. Ba^{2+} ions and water molecules are located at the interlayer space. The Ba^{2+} cation is ten coordinated by nine oxygen atoms from two neighboring galloborate layers as well as a water molecule with Ba–O distances ranging from 2.699(6) to 3.063(5) Å (Figure S2 in the ESI†). The calculated total bond valances for Ba(1), Ga(1), B(1)–B(4) atoms are 2.18, 3.06, 3.06, 3.07, 2.98, 3.04, respectively, indicating that Ba, Ga and B atoms are in oxidation states of +2, +3 and +3, respectively.[28] There are hydrogen bonds among water molecule, hydroxyl group and oxygen atoms of the borate cluster (O(1W)–H(1WA)···O(3) 2.696 Å; O(1)–H(8A)···O(2) 2.700 Å) (Table S2 in the ESI†) which provide additional stability for the structure.

<Figure 1 here>

The overall structures of the *α*– and *β*–forms of $BaGa[B_4O_8(OH)](H_2O)$ are quite similar.[19] However some differences do exist. Firstly, they belong to two different crystal systems and space groups; secondly, the 2D galloborate layers are packed in different fashions along the *c*–axis. The *β*– and *α*–phases contain one and two repeated galloborate layers within their unit cells, respectively, hence the length of the *c* axis for *α*-phase is almost doubled compared with that of the *β*–form.

The structure of compound **1** is also closely related with that of $K_4[Ge_2B_8O_{17}(OH)_2]$.[21b] In $K_4[B_8Ge_2O_{17}(OH)_2]$, the 2D borogermanate layer is based on $[B_4O_8(OH)]^{5-}$ unit and $[Ge_2O_7]^{6-}$ dimer formed by two GeO_4 tetrahedra. However, $[B_4O_8(OH)]^{5-}$ unit in $K_4[B_8Ge_2O_{17}(OH)_2]$ has a different shape from that in compound **1**. The BO_3 group is no longer hanging on the B_3O_7 group but bridges with two B atoms of the B_3O_7 group, hence $[B_4O_8(OH)]^{5-}$ unit in $K_4[B_8Ge_2O_{17}(OH)_2]$ forms two orthogonal B_3O_8 groups.

$Ba_4Ga[B_{10}O_{18}(OH)_5](H_2O)$ (**2**) crystallizes in the polar space group *Cc*. Its structure consists of a unique 3D network composed of $[B_{10}O_{18}(OH)_5]^{11-}$ clusters and $[GaO_4]^{5-}$ tetrahedra that are interconnected via Ga–O–B linkages, forming large 1D tunnels of Ga_3B_{16} rings which are filled by Ba^{2+} ions and water molecules (Figure 2d). The asymmetric unit of $Ba_4Ga[B_{10}O_{18}(OH)_5](H_2O)$ (**2**) consists of four Ba^{2+}, one Ga^{3+}, one $[B_{10}O_{18}(OH)_5]^{11-}$ cluster and a water molecule. Within the $[B_{10}O_{18}(OH)_5]^{11-}$ anion, B(1), B(7), and B(9) atoms form planar trigonal BO_3 groups whereas the remaining B atoms are tetrahedrally coordinated. For the BO_3 groups, the B–O distances are in the range of 1.356(7)–1.399(7) Å and O–B–O bond angles range from 113.8(5)–123.9(5)°. B–O distances and O–B–O angles for the BO_4 tetrahedra are in the range of 1.429(6)–1.554(7) Å and 105.3(4)–115.7(5)°, respectively. The Ga^{3+} ion is tetrahedrally by four oxygen atoms from two [BO_3] and two [BO_4] groups from four different $[B_{10}O_{18}(OH)_5]^{11-}$ clusters (Figure 2b). The Ga–O bond distances and O–Ga–O bond angles are in the range of 1.806(4)–1.869(4) Å and 103.6(5)–112.5(8)°, respectively. These bond lengths and angles are comparable to those reported in *α*– and *β*–forms of $BaGa[B_4O_8(OH)](H_2O)$ and other galloborates previously reported.[18-20]

$[B_{10}O_{18}(OH)_5]^{11-}$ cluster in $Ba_4Ga[B_{10}O_{18}(OH)_5](H_2O)$ is quite novel. It can be considered to be formed by a central B_6O_{14} cluster corner–sharing with a B_3O_8 cluster and a $B(1)O_3$ group in both ends (Figure 2a). The central B_6O_{14} cluster consists of three 3–MRs, the middle one is formed by three BO_4 groups whereas the other two are formed by two BO_4 and one BO_3 groups. O(5), O(6), O(11), O(13) and O(23) atoms are protonated. To the best of our knowledge, such type of borate cluster has not been reported before.

<Figure 2 here>

The interconnection of $[B_{10}O_{18}(OH)_5]^{11-}$ clusters and GaO_4 tetrahedra via corner-sharing led to a novel 3D network (Figure 2c). Each $[B_{10}O_{18}(OH)_5]^{11-}$ polyanion connects with four GaO_4 tetrahedra *via* corner–sharing (O(1), O(17), O(19) and (O22)) and each GaO_4 also connects with four $[B_{10}O_{18}(OH)_5]^{11-}$ clusters. Such connectivity resulted in the formation of a large 1D tunnels based on Ga_3B_{16} 19–MRs along the *a* axis. Each Ga_3B_{16} ring consists of three GaO_4, five BO_3 and eleven BO_4 groups. The tunnels are filled by Ba^{2+} cations and water molecules. Ba(1) and Ba(3) atoms are ten coordinated by ten oxide anions whereas Ba(2) and Ba(4) atoms are nine-coordinated by eight oxide anions and a water molecules (Figure S3 in the ESI†). The Ba–O distances are in the range of 2.652(4)–3.180(4) Å. The calculated total bond valances for Ba1–Ba4, Ga1 are 2.04, 1.78, 2.40, 1.92, 3.02, respectively, and those for B1 to B10 are 3.01, 3.03, 3.03, 3.02, 3.02, 3.06, 3.06, 3.05, 3.05, 3.07, respectively, indicating that Ba, Ga and B are in oxidation states of +2, +3, and +3, respectively.[28]. The water molecule and hydroxyl groups of the borate cluster are involved in hydrogen bonding which provides additional stability for the network structure (Table S2 in the ESI†).

It is interesting to compare the structure of $Ba_4Ga[B_{10}O_{18}(OH)_5](H_2O)$ with that of $Ba_3Ga_2[B_3O_6(OH)]_2[B_4O_7(OH)_2]$ which contains two different types of borate clusters. The structure of $Ba_3Ga_2[B_3O_6(OH)]_2[B_4O_7(OH)_2]$ exhibits a 3D network structure with 14-MR channels along the [100], [101], and [-101] directions based on GaO_4 tetrahedra, $B_3O_6(OH)$ and $B_4O_7(OH)_2$ clusters.[20]

Optical properties. *β*–$BaGa[B_4O_8(OH)](H_2O)$ (**1**) and $Ba_4Ga[B_{10}O_{18}(OH)_5](H_2O)$ (**2**) show strong absorption in the region of 200 to 370 nm and 200 to 418 nm, respectively (Figure S4 in the ESI†). Both compounds show little absorption in the range of 420–2000 nm. Optical diffuse reflectance spectra reveal that compounds **1** and **2** are wide band gap semiconductors with optical band gaps around 4.65 and 4.12 eV, respectively (Figure S5 in the ESI†). Both compounds display absorption broad IR absorption bands at 3615, 3439 and 3264 cm^{-1} due to the presence of OH groups and H_2O molecules. For compound **1**, the absorption band at 1679 cm^{-1} is also assigned to the asymmetric stretching vibrations and symmetric bond–bending vibrations of O–H bonds. The vibration absorption bands at 1410–1220 cm^{-1} are due to B–O bond asymmetric stretching of the BO_3 units, whereas those of BO_4 units appeared at 1085–921 cm^{-1}. The peaks at 658 and 740 cm^{-1} are due to the stretching vibration of GaO_4 (Figure S6a in the ESI†). Similar to compound **2**, the absorption bands at 1240–1350 and 856 cm^{-1} can be assigned to the asymmetric stretch vibrations of the BO_3 groups. The absorption peak at 1033 cm^{-1} can be assigned to the asymmetric stretch vibrations of the BO_4 group. The absorption peak at around 961 cm^{-1} are due to the symmetric stretch vibrations of the BO_3 group. The absorption bands at 770−808 cm^{-1} can be assigned to the symmetric stretch vibrations of BO_4 group (Figure S6b in the ESI†). The absorption bands with frequency below 600 cm^{-1} are difficult to be assigned undoubtedly due to the overlaps of the bending modes of BO_4 and GaO_4 polyhedron in the low frequency vibrations. These assignments are in agreement with those reported in other barium galloborates.[18-20]

TGA and DSC studies. Thermogravimetric analysis (TGA) studies indicate that *β*–$BaGa[B_4O_8(OH)](H_2O)$ (**1**) shows a weight loss in the range of 300–650 °C under nitrogen atomosphere, which corresponds to the removal of 1.5 mol of water molecules per formula unit, and one endothermic peak at around 423 °C can be found in the DSC curve. The observed weight loss of 6.55% matches well with the calculated one (6.53%) (Figure S7a in the ESI†). The endothermic peak at 817 °C corresponds to the melting of the dehydrated product. $Ba_4Ga[B_{10}O_{18}(OH)_5](H_2O)$ (**2**) displays one step of weight loss in the range of 480–600 °C, which corresponds to release of 3.5 mol of H_2O molecules per formula unit. The observed weight loss of 5.63% is in agreement with the calculated one (6.03%) (Figure S7b in the ESI†). This assignment is also in agreement with the endothermic peak at 504 °C in the DSC curve. The endothermic peak at 790 °C corresponds to the melting of the dehydrated product. $Ba_3Ga_2[B_3O_6(OH)]_2[B_4O_7(OH)_2]$ and *α*–$BaGa[B_4O_8(OH)](H_2O)$ can keep stable under 400 °C and 350 °C, respectively. Because *α*/*β*–$BaGa[B_4O_8(OH)](H_2O)$ have similar structures, their stability are simialar. And there exit more hydrogen bonds in $Ba_3Ga_2[B_3O_6(OH)]_2[B_4O_7(OH)_2]$ and compound **2** comparing with that in *α*/*β*–$BaGa[B_4O_8(OH)](H_2O)$. So their stability is better than *α*/*β*–$BaGa[B_4O_8(OH)](H_2O)$**.** The residues obtained after thermal annealing (at 700 °C for 5 h) of two compounds are characterized by powder X-ray diffraction patterns which shows they may be new pahses. (Figure S1c and S1d in the ESI†). It may be reported in later work.

SHG properties. Since $Ba_4Ga[B_{10}O_{18}(OH)_5](H_2O)$ (**2**) crystallizes in the polar space group *Cc*, it is worthy to study their SHG properties. SHG measurements on a 1064 nm Q–switched Nd:YAG laser with the sieved crystal samples (100–150 μm) reveal that it displays weak SHG responses of 0.2 times that of KDP (Figure 3).

<Figure 3 here>

According to the anionic–group theory, its SHG signal may mainly originate from the BO_3 groups and small contribution from BO_4 groups.[29] Taking this approximation and neglecting the contribution from those Ba–coordinated polyhedra, the local dipole moments for the GaO_4, BO_3 and BO_4 polyhedra and the net dipole moment within a unit cell were calculated by using a method reported earlier.[30] The calculated dipole moments for the GaO_4, BO_4 and BO_3 groups are 1.17 D, 0.84–2.14 D, and 0.98–1.46 D, respectively, which is agreement with previously reported values (Table S3 in the ESI†). The net dipole moment for a unit cell was calculated to be a relative small value of 13.44 D. Hence, in compound **2**, the weak SHG response could be mainly attributed to three factors. Firstly, due to the little distortions, it is very weak of the contributions from GaO_4 tetrahedra. Secondly, the BO_4 groups produce small second–order susceptibility. And lastly, the polarizations produced by BO_4 and BO_3 groups largely cancel each other out.

Ferroelectric and piezoelectric properties. The ferroelectric property of $Ba_4Ga[B_{10}O_{18}(OH)_5](H_2O)$ (**2**) was investigated because the crystal structure is in a polar space group (*Cc*) required for ferroelectric behavior. Ferroelectric measurements on pellets for $Ba_4Ga[B_{10}O_{18}(OH)_5](H_2O)$ (**2**) (5–mm–diameter and 0.4–mm–thick) showed 'polarization loops' which were frequency dependence and ferroelectric measurements revealed a very small remanent polarization (Pr) of 0.10 μC/cm^2 and a saturation spontaneous polarization (Ps) of 0.20 μC/cm^2 (Figure S8 in the ESI†). Due to these coefficients are very small, its ferroelectric property is negligible.[5d] After the sample was poled at electric field of 1.5 Ec, piezoelectric property of **2** was investigated and piezoelectric coefficient d_{33} was measured to be 3 pC/N.

Theoretical studies. To further understand the electronic structures of both compounds, theoretical calculations based on DFT methods were performed. The calculated band structures of β–$BaGa[B_4O_8(OH)](H_2O)$ (**1**) and $Ba_4Ga[B_{10}O_{18}(OH)_5](H_2O)$ (**2**) along high symmetry points of the first Brillouin zone are plotted in Figure 4, and the state energies (electronvolts) of the lowest conduction band (LCB) and the highest valence band (HVB) of both compounds are listed in Table S4. For the compound **1**, the minimum of LCB is localized at G point, whereas the maximum of HVB is localized between Z and G point, displaying an indirect band gap of 5.17 eV. For compound **2**, the minimum of LCB is localized at G point and the maximum of HVB is localized between E and C point, revealing an indirect band gap of 4.29 eV. The calculated band gaps are close to experimental values (4.65 and 4.12 eV for **1** and **2**, respectively).

<Figure 4 here>

The bands can be assigned according to the total and partial DOS, as plotted in Figure 5. We take β–$BaGa[B_4O_8(OH)](H_2O)$ (**1**) as a representative to describe them in detail, owing to the similarity between the two compounds. For compound **1**, the valence band ranging from –21.0 to –16 eV arises from mostly O–2s, mixing with a small amount of B–2s2p and H–1s states. The band around –13 eV is mostly contributed from Ga–3d states, and the band around –10 eV is mostly contributed by Ba–5p. In the vicinity of the Fermi level, namely, from –10.5 to 0 eV in the valence band and from 4.8 to 13.6 eV in the conduction band, the O–2p, B–2s2p, Ga–4s4p, and H–1s states are all involved and overlap fully among them.

<Figure 5 here>

Population analyses give more information about quantitative bond analysis. The calculated bond orders of Ga–O, H–O bonds are 0.24–0.37 e, 0.58–0.61 e and 0.66–0.90 e, 0.34–0.65 e for B–O in BO_3 and BO_4 groups, respectively, for β–BaGa $[B_4O_8(OH)](H_2O)$ (**1**), whereas for $Ba_4Ga[B_{10}O_{18}(OH)_5](H_2O)$ (**2**), the calculated bond orders are 0.36–0.45 e, 0.59–0.69 e for Ga–O, H–O bonds and 0.76–0.85 e, 0.49–0.70 e for B–O in BO_3 and BO_4 groups, respectively. So we can say that the B–O bonds are stronger than Ga–O bonds in two compounds.

Conclusion

In summary, two new barium galloborates, namely β–$BaGa[B_4O_8(OH)](H_2O)$ (**1**) and $Ba_4Ga[B_{10}O_{18}(OH)_5](H_2O)$ (**2**) have been prepared by changing starting materials and stoichiometric ratios, and structurally characterized. They adopt two different anionic open frameworks based on polymeric borate clusters and GaO_4 (or $[Ga_2O_8]^{10-}$) groups. Compound **1** displays a two-dimensional (2D) layer anionic framework composed of $[B_4O_8(OH)]^{5-}$ clusters and $[Ga_2O_8]^{10-}$ dimers. Compound **2** crystallizes in a polar space group *Cc* and features a 3D network composed of $[B_{10}O_{18}(OH)_5]^{11-}$ clusters and $[GaO_4]^{5-}$ tetrahedra forming large 1D tunnels based on Ga_3B_{16} 19–MRs that accommodate the Ba^{2+} cations and H_2O moleculars. Compound **2** shows a weak SHG response of 0.2 times that of KDP. The results of our studies indicate that even in a same system, subtle changes of reaction conditions can lead to many different phases with different structures. Our future research efforts will be devoted to the preparation of other boron–rich or galluim–rich metal galloborates with interesting structures and physical properties.

Ackowledgements

This work was supported by National Natural Science Foundation of China (Grants 21231006, 21373222, and 21001107).

Notes and references

[a] *State Key Laboratory of Structural Chemistry, Fujian Institute of Research on the Structure of Matter, Chinese Academy of Sciences, Fuzhou 350002, P. R. China*
[b] *University of the Chinese Academy of Sciences, Beijing 100039, P. R. China*
FAX: (+86)591-83714946; Tel: (86)591-83704836;
E-mail: mjg@fjirsm.ac.cn

† Electronic Supplementary Information (ESI) available: X–ray crystallographic files in CIF format, simulated and experimental XRD powder patterns, dipole moment calculations, the calculated state energies of the L-CB and H-VB, hydrogen bond, IR spectra, UV spectra, optical diffuse reflectance, TGA and DSC curves, ferroelectric properties data, coordination environments around the Ba atoms for both compounds. CSD reference numbers 427785, 427786. See DOI: 10.1039/b000000x/

1 (a) K. M. Ok, E. O. Chi and P. S. Halasyamani, *Chem. Soc. Rev.*, 2006, **35**, 710; (b) C. T. Chen, G. Z. Liu, *Annu. Rev. Mater. Sci.*, 1986, **16**, 203.
2 T. Sasaki, Y. Mori, M. Yoshimura, Y. K. Yap and T. Kamimura, *Mater. Sci. Eng. Rep.*, 2000, **30**, 1.
3 (a) P. Becker, *Adv. Mater.*, 1998, **10**, 979; (b) M. E. Hagerman, K. R. Poeppelmeier, *Chem. Mater.*, 1995, **7**, 602; (c) B. C. Wu, D. Y. Tang, N. Ye and C. T. Chen, *Optical Materials*, 1996, **5**, 105.

4 M. Touboul, N. Penin and G. Nowogrocki, S*olid State Sci*, 2003, **5**, 1327.

5 (a) M. S. Dadachov, K. Sun, T. Conradsson and X. D Zou, *Angew. Chem., Int. Ed.*, 2000, **39**, 3674; (b) Y. F. Li, X. D. Zou, *Angew. Chem., Int. Ed.*, 2005, **44**, 2012; (c) H. X. Zhang, J. Zhang, S. T. Zheng and G. Y. Yang, *Inorg. Chem.*, 2005, **44**, 1166; (d) J. H. Zhang, F. Kong and J. G. Mao, *Inorg. Chem.*, 2011, **50**, 3037; (e) X. Xu, C. L. Hu, F. Kong, J. H. Zhang and J. G. Mao, *Inorg. Chem.*, 2011, **50**, 8861.

6 (a) S. C. Sevov, *Angew. Chem., Int. Ed. Engl.*, 1996, **35**, 2630; (b) R. Kniep, H. Engelhardt and C. Hauf, *Chem. Mat*er., 1998, **10**, 2930.

7 (a) J. Zhou, W. H. Fang, C. Rong and G. Y. Yang,. *Chem. Eur. J.*, 2010, **16**, 4852; (b) T. Yang, A. Bartoszewicz, J. Ju, J. L. Sun, Z. Liu, X. D. Zou, Y. X. Wang, G. B. Li, F. H. Liao, B. Martin-Matute and J. H. Lin, *Angew. Chem. In. Ed.*, 2011, **50**, 12555.

8 H. A. Höppe, K. Kazmierczak, M. Daub, K. Förg, F. Fuchs and H. Hillebrecht, *Angew. Chem.*, 2012, **124**, 6359; *Angew. Chem., Int. Ed.*, 2012, **51**, 6255.

9 (a) S. C. Wang, N. Ye, W. Li and D. Zhao, *J. Am. Chem. Soc.*, 2010, **132**, 8779; (b) X. Yan.; S. Y. Luo, Z. S. Lin, Y. C. Yue, X. Y. Wang, L. J. Liu and C. T. Chen. *J. Mater. Chem. C.*, 2013, **1**, 3616.

10 T. Hu, C. L. Hu, F. Kong, J. G. Mao and T. W. Mak, *Inorg. Chem.***,** 2012, **51**, 8810.

11 Z. H. Liu, P. Yang and P. Li, *Inorg. Chem.*, 2007, **46**, 2965.

12 R. W. Smith, M. A. Kennard and M. J. Dudik, *Materials Research Bulletin*, 1997, **32**, 649.

13 R. W. Smith, C. H. Hu and C. D. DeSpain, *Acta Crys*t, 2008, **E64**, i23.

14 G. K. Abdullaev, Kh. S. Mamedov, *Zhurnal Strukturnoi Khimii*, 1972, **13**, 943.

15 Z. Yang, X. L. Chen, J. K. Liang, Y. C. Lan and T. Xu, *Journal of Alloys Compd*, 2001, **319**, 247.

16 (a) Z. Yang, X. L. Chen, J. K. Liang, M. He and J. R. Chen, *Crystal Research and Technology*, 2004, **39**, 634; (b) Z. Yang, J. K. Liang, X. L. Chen, T. Xu and Y. P. Xu, *Journal of Alloys Compd*, 2001, **327**, 215.

17 Z. Yang, J. K. Liang, X. L. Chen and J. R. Chen, *J. Solid State Chem.*, 2002, ***165***, 119.

18 H. Park, J. Barbier, *J. Solid State Chem.*, 2000, **154**, 598.

19 Q. Wei, L. Li, L. Cheng, Q. Meng and G. Y. Yang, *Dalton Trans.*, 2014, DOI:10.1039/C4DT00652F.

20 L. Cheng, Q. Wei, H. Q. Wu, L. J. Zhou, G. Y. Yang, *Chem. Eur. J.*, 2013, **19**, 17662.

21 (a) H. X. Zhang, J. Zhang, S. T. Zheng, G. M. Wang and G. Y. Yang, *Inorg. Chem.*, 2004, **43**, 4168; (b) D. B. Xiong, J. T. Zhao, H. H. Chen and X. X. Yang, *Chem. Eur. J.*, 2007, **13**, 9862; (c) Z. E. Lin, J. Zhang and G. Y. Yang, *Inorg. Chem.*, 2003**, 42**, 1797.

22 W. M. Wendlandt, H. G. Hecht, *Reflectance Spectroscopy; Interscience*: New York, 1966.

23 S. W. Kurtz,; T. T. Perry, *J. Appl. Phys.*, 1968, **39**, 3798.

24 (a) CrystalClear, version 1.3.5; *Rigaku Corp.: Woodlands, TX*, 1999; (b) G. M. Sheldrick, SHELXTL, Crystallographic Software Package, version 5.1; *Bruker-AXS: Madison, WI,* 1998; (c) A. L. Spek, *PLATON*; Utrecht University: Utrecht, The Netherlands, 2001.

25 (a) M. D. Segall, P. J. D. Lindan, M. J. Probert, C. J. Pickard, P. J. Hasnip, S. J. Clark and M. C. Payne, *J. Phys.: Condens. Matt.*, 2002, **14**, 2717; (b) V. Milman, B. Winkler, J. A. White, C. J. Pickard, M. C. Payne, E. V. Akhmatskaya and R. H. Nobes, *Int. J. Quantum Chem.*, 2000, **77**, 895.

26 J. P. Perdew, K. Burke, M. Ernzerhof, *Phys. Rev. Lett.*, 1996, **77**, 3865.

27 J. S. Lin, A. Qteish, M. C. Payne and V. Heine, *Phys. Rev. B.*, 1993, **47**, 4174.

28 (a) I. D. Brown, D. Altermatt, *Acta Cryst.,* 1985, **B41**, 244. (b) N. E. Brese, M. ÖKeeffe, *Acta Cryst.*, 1991, **B47**, 192.

29 (a) C. T. Chen, Y. C. Wu, R. C. Li, *J. Cryst. Growth.*, 1990, **99**, 790; (b) H. Yu, H. Wu, S. Pan, Z. Yang, X. Su and F. Zhang, *J. Mater. Chem.*, 2012, **22**, 9665; (c) Y. Yang, S. Pan, J. Han, X. Hou, Z. Zhou, W. Zhao, Z. Chen and M. Zhang, *Cryst. Growth Des.*, 2011, **11**, 3912; (d) C. L. Hu, X. Xu, C. F. Sun and J. G. Mao, J. *Phys.: Condens. Matter.*, 2011, **23**, 395501.

30 (a) H. Y. Li, H. P. Wu, X. Su, H. W. Yu, S. L. Pan, Z. H. Yang, Y. Lu, J. Han and K. R. Poeppelmeier, *J. Mater. Chem.*, 2014, **2**, 1704; (b) Y. J. Shi, S. L. Pan, X. Y. Dong, Y. Wang, M. Zhang, F. F. Zhang and Z. X. Zhou, *Inorg. Chem.*, 2012, **51**, 10870; (c) H. K. Izumi, J. E. Kirsch, C. L. Stern and K. R. Poeppelmeier, *Inorg. Chem.*, 2005, **44**, 884.

Table 1. Crystal data and structure refinements for β–BaGa[B_4O_8(OH)](H_2O) (**1**) and Ba_4Ga[$B_{10}O_{18}(OH)_5$](H_2O) (**2**)

Formula	β-BaGa(B_4O_8(OH))(H_2O)(**1**)	$Ba_4Ga(B_{10}O_{18}(OH)_5)(H_2O)$(**2**)
Fw	413.32	1118.24
Space group	*P*-1	*Cc*
a [Å]	7.0811(6)	7.0097(3)
b [Å]	7.1144(7)	12.2089(5)
c [Å]	9.8431(8)	22.5507(9)
α [º]	106.946(8)	90
β [º]	91.245(7)	96.798(4)
γ [º]	119.145(9)	90
V [$Å^3$]	406.26(6)	1916.34(14)
Z	2	4
D_{calcd}[$g\cdot cm^{-3}$]	3.379	3.876
μ [mm^{-1}]	8.174	9.612
F(000)	380	2016
GOF on F^2	1.111	1.017
R1, *w*R2 ($I>2\sigma(I)$)[a]	0.0386, 0.0922	0.0212, 0.0414
R1, *w*R2 (all data)	0.0425, 0.0982	0.0221, 0.0418

[a] $R1 = \sum||F_o| - |F_c||/\sum|F_o|$, $wR2 = \{\sum w[(F_o)^2 - (F_c)^2]^2/\sum w[(F_o)^2]^2\}^{1/2}$

Figure captions

Figure 1. A $[B_4O_8(OH)]^{5-}$ unit (a), a $[Ga_2O_8]^{10-}$ group (b), a 2D $[GaB_4O_8(OH)]^{2-}$ layer parallel to the *ab* plane (c), and view of the structure of *β*-$BaGa[B_4O_8(OH)](H_2O)$ (**1**) along the *b* axis. The B, Ba, and O atoms are drawn as purple, yellow, and red circles, respectively. GaO_4 tetrahedra are shaded in cyan.

Figure 2. A $[B_{10}O_{18}(OH)_5]^{11-}$ unit (a), a GaO_4 group (b), view of the 3D galloborate anionic strcuture down the *a* axis (c), and view of the structure of $Ba_4Ga[B_{10}O_{18}(OH)_5](H_2O)$ (2) down the *a* axis. The B, Ba, and O atoms are drawn as purple, yellow, and red circles, respectively. GaO_4 tetrahedra are shaded in cyan.

Figure 3. Oscilloscope traces of SHG signals for the powders (100–150 μm) of KDP and $Ba_4Ga[B_{10}O_{18}(OH)_5](H_2O)$ (**2**).

Figure 4. Calculated band structure of *β*-$BaGa[B_4O_8(OH)](H_2O)$ (**1**) (a) and $Ba_4Ga[B_{10}O_{18}(OH)_5](H_2O)$ (**2**) (b).

Figure 5. .Electronic DOS curves for *β*-$BaGa[B_4O_8(OH)](H_2O)$ (**1**) (a) and $Ba_4Ga[B_{10}O_{18}(OH)_5](H_2O)$ (**2**) (b)

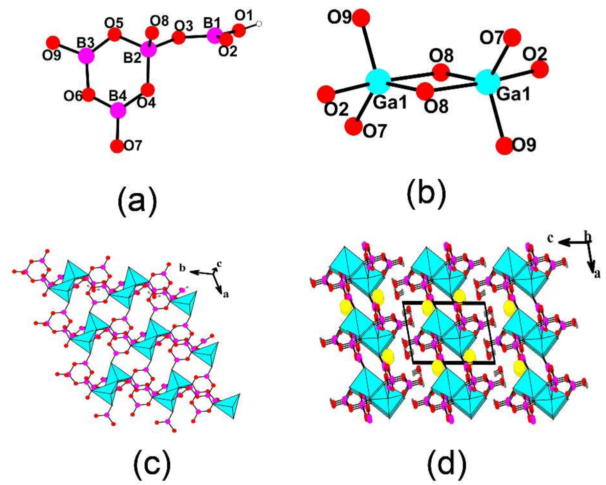

Figure 1

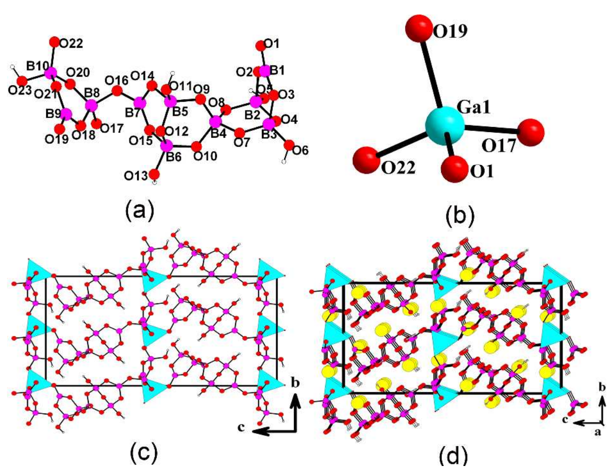

Figure 2

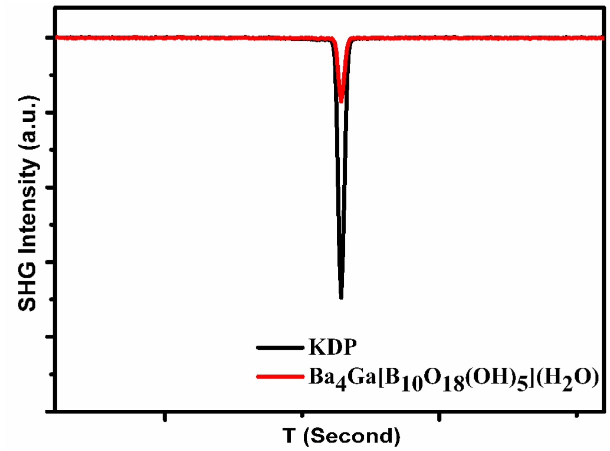

Figure 3

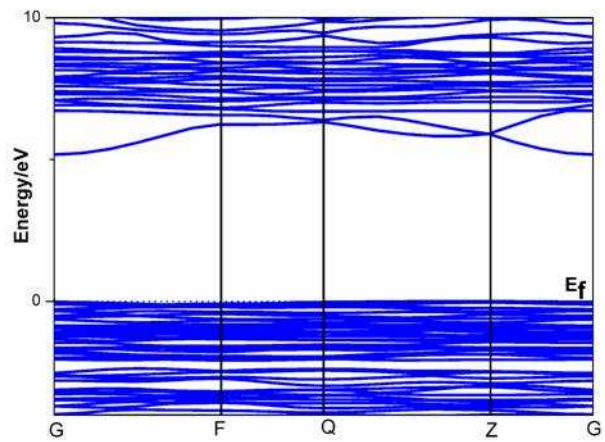

(a)

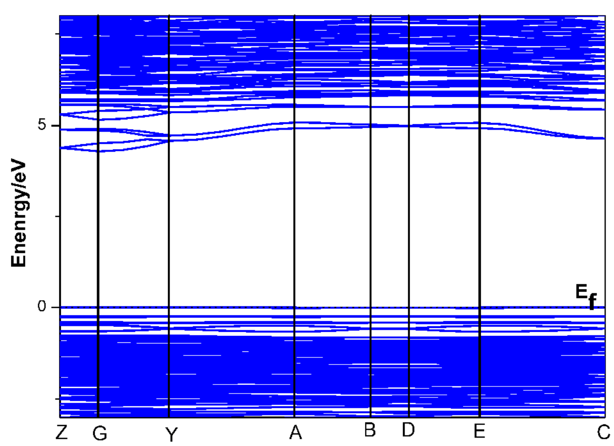

(b)

Figure 4

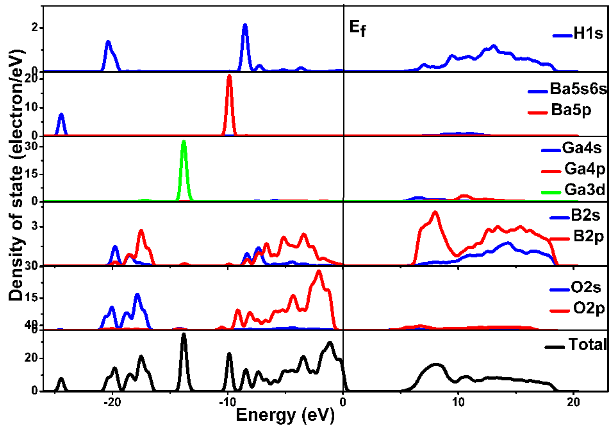
Ef
H1s
Ba5s6s
Ba5p
Ga4s
Ga4p
Ga3d
B2s
B2p
O2s
O2p
Total
Density of state (electron/eV)
Energy (eV)

(a)

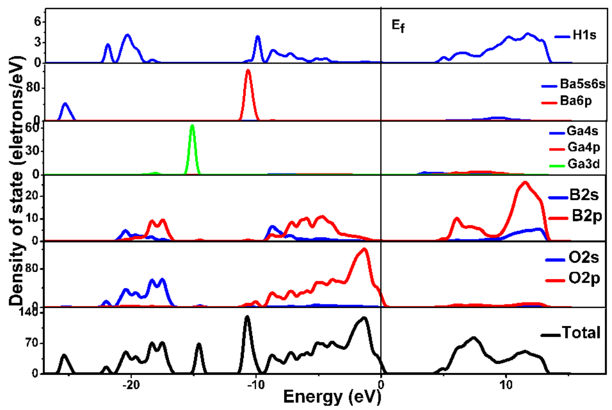
Ef
H1s
Ba5s6s
Ba6p
Ga4s
Ga4p
Ga3d
B2s
B2p
O2s
O2p
Total
Density of state (eletrons/eV)
Energy (eV)

(b)

Figure 5